A Biocompatible Thermoset Polymer Binder for Direct Ink Writing of Porous Titanium Scaffolds for Bone Tissue Engineering

Yunhui Chen*[a,g,h], Pingping Han[b], Luigi-Jules Vandi[c], Ali Dehghan-Manshadi[a], Jarrad Humphry[e], Damon Kent[a,d,f], Ilaria Stefani[b], Peter Lee [g,h], Michael Heitzmann[e], Justin Cooper-White[b], Matthew Dargusch[a,d]

a. Queensland Centre for Advanced Materials Processing and Manufacturing (AMPAM), The University of Queensland, St. Lucia, 4072, Australia

b. The UQ Centre in Stem Cell Ageing and Regenerative Engineering (StemCARE), Australian Institute for Bioengineering and Nanotechnology, The University of Queensland, St. Lucia, 4072, Australia

c. School of Chemical Engineering, Faculty of Engineering, Architecture and Information Technology, The University of Queensland, St. Lucia, 4072, Australia

d. ARC Research Hub for Advanced Manufacturing of Medical Devices

e. School of Mechanical and Mining Engineering, Faculty of Engineering, Architecture and Information Technology, The University of Queensland, St. Lucia, 4072, Australia

f. School of Science and Engineering, University of the Sunshine Coast, Maroochydore DC, QLD 4558, Australia

g. School of Mechanical Engineering, University College London, Torrington Place, London, WC1E 7JE

h. Research Complex at Harwell, Rutherford Appleton Laboratory, Didcot, OX11 0FA

*Corresponding author: Yunhui Chen

y.chen18@uq.edu.au

Abstract

There is increasing demand for synthetic bone scaffolds for bone tissue engineering as they can counter issues such as potential harvesting morbidity and restrictions in donor sites which hamper autologous bone grafts and also address the potential for disease transmission in the case of allografts. Due to their excellent biocompatibility, titanium scaffolds have great potential as bone graft substitutes as they can mimic the structure and properties of human cancellous bone. Here we report on a new thermoset bio-polymer which can act as a binder for Direct Ink Writing (DIW) of titanium artificial bone scaffolds. We demonstrate the use of the binder to manufacture porous titanium scaffolds with evenly distributed and highly interconnected pores ideal for orthopaedic applications. Due to their porous titanium structure, the scaffolds exhibit an effective Young's modulus similar to human cortical bone, alleviating undesirable stress-shielding effects, and possess superior strength. The biocompatibility of the scaffolds was investigated in vitro by cell viability and proliferation

assays using human bone-marrow-derived Mesenchymal stem cells (hMSCs). The hMSCs displayed well-spread morphologies, well-organised F-actin and large vinculin complexes confirming their excellent biocompatibility. The vinculin regions had significantly larger Focal Adhesion (FA) area and equivalent FA numbers compared to that of tissue culture plate (TCP) controls, showing that the scaffolds can support cell viability and promote attachment. In conclusion, we have demonstrated the excellent potential of thermoset bio-polymer as a Direct Ink Writing ready inkjet binder for manufacture of porous titanium scaffolds for hard tissue engineering.

Keywords: Direct Ink Writing (DIW), Binder, Biocompatible scaffold, Tissue Engineering, Titanium, Additive Manufacturing

Statement of Significance

For the first time, a thermoset biopolymer is introduced as a binder to create an 'ink' appropriate for extrusion printing for Direct Ink Writing (DIW) of titanium powders. The binder is then removed during the furnace sintering process used to consolidate the part. This concept exhibits a huge potential as it solves a fundamental limitation in metallic 3D printing, i.e. controlled printing of complex parts at micrometre scales and avoids issues associated with highly localised heating and cooling. The method enables zero-waste fabrication of high value materials, with no limit to the selection of metallic material. In our study, this innovation enabled production of scaffolds which held their shape during sintering with minimal shrinkage. This is a ground-breaking concept for metallic 3D printing as it enables DIW of artificial skeletal implants for the repair of damaged bone. The porous scaffolds mimic the mechanical performance and density of cancellous bone, addressing the primary causes of implant loosening by matching the implant stiffness to bone. *In-vitro* stem cell culture tests show that the scaffolds provide ideal conditions for adhesion and proliferation.

1. Introduction

Synthetic scaffolds hold great promise as a new approach to repair and remodel damaged bone tissue as they remove the potential for disease transmission from donor to recipient as can occur for traditional allografts [1]. They can also counter limitations in the use of autografts such as restricted donor sites, possible harvesting morbidity, and unpredictable resorption [2,3]. Titanium and its alloys are widely used in the fields of orthopaedic [4] and dental implants due to their excellent mechanical properties, corrosion resistance, and biocompatibility [5,6]. Porous titanium scaffolds are an exceptional candidate for bone graft substitutes due to their porous framework which mimics cancellous bone [7–10]. These porous titanium structures can be produced by a variety of processes such as solid-state foaming [11], chemical vapour deposition (CVD) on cellular preforms [12], and powder metallurgy processing techniques [13].

Chen *et al.* [13,14] demonstrated a powder metallurgy approach to develop porous titanium scaffolds using temporary space holder materials to generate porous structures with high pore sphericity. The mechanical properties of the scaffolds closely matched human cortical bone and supported osteoblast adhesion and cell spreading. A significant limitation was an inability to effectively control the structure to the extent necessary for optimal mechanical performance and osseointegration of implants. On the other hand, additive manufacturing technologies including Selective Laser Melting (SLM), Electron Beam Melting (EBM), Direct Metal Laser Sintering (DMLS) and Laser Engineered Net Shaping (LENS) can be used to fabricate open cell porous titanium scaffolds with greater levels of control [15]. However, they employ high localised energy inputs to melt the metal powder, resulting in steep temperature gradients and rapid cooling which give rise to undesirable and inhomogeneous microstructures and impart significant residual stresses which can reduce

mechanical performance. Due to restrictions in the powder size which can be employed (typically ≥45 um) and in constraining the interaction with the energy source due to high heat dissipation in metals, it is very difficult to produce intricate and fine-scale features at or below the scale of the powder. Minimum feature sizes are typically in the order of a few tens of micrometres [16]. Other issues such as unintended porosity, balling defects and incorporation of unmelted particles can compromise the structural integrity [17]. For intricate and fine-scale features it is extremely difficult and/or impossible to completely remove unmelted powder, such as in the case of closed cell porous structures. Loose or partially sintered powder may present potential inflammatory or toxicity concerns for patients [18] Hence, for scaffolds produced by these methods feature sizes must generally be significantly larger than the feed powder, typically in the order of 1 mm [19] with an open cell design. Additionally, for technologies utilising a powder bed such as SLM and EBM, there are significant issues with recycling of used powders so that these methods cannot reliably deliver waste-free manufacture [20].

Direct Ink Writing (DIW) was introduced by Lewis *et al.* [21] as a new additive manufacturing approach enabling high resolution fabrication of geometrically complex net-shape parts. Its benefits include excellent geometric and dimensional control and zero-waste of high value materials [18]. The fabrication process involves the use of DIW to form a green part which is then consolidated by conventional furnace sintering. The process avoids issues arising from high localised temperatures encountered in other metallic '3D printing' or additive manufacturing technologies. DIW enables fabrication of intricate and fine-scale features, coupled with uniform and controlled heating and cooling of the part during sintering. According to Hirt *et al.*, DIW can enable production of metals with feature sizes in the range of 0.6-30 µm [16].

To date, DIW of polymers and ceramics has been investigated most extensively and was

successfully demonstrated for manufacture of ceramic scaffolds for hard tissue implants [22]. However, DIW of metals is currently confined to silver nanoparticles [16]. Colloidal and nanoparticle based inks, polyelectrolyte inks and sol-gel inks are some typical binders used for DIW [23]. Jakus *et al.* [24] employed particle-based inks which hardened upon extrusion due to rapid evaporation of solvent and subsequent precipitation of a binding polymer but the authors noted that the production process was difficult due to the lengthy solidification time. Although complete densification was not achieved, it was noted that porosity is potentially desirable for applications such as biomedical implants.

In the present study, sintering of titanium in the presence of a thermoset pine-oil-based bio-epoxy has been evaluated with the aim to establish its suitability as a novel inkjet binder for DIW of titanium for orthopaedic scaffolds. The thermoset polymer ink allows the scaffold to hold its shape during sintering, enabling production of complex porous structures appropriate for hard tissue engineering. The scaffolds show abundant open porosity and remarkable compressive strength, coupled with favourable biological properties that promote cell proliferation. This manufacturing method has significant potential for rapid net shape manufacturing of metallic biomedical parts, especially for orthopaedic applications requiring intricate and fine-scale features.

2. Experimental procedure

2.1 Sample preparation

SUPER SAP Epoxy Systems (manufactured by Entropy Resins), a pine-oil-based bio-epoxy, was used in this study as a binder. Resin and hardener were mixed with volume ratio of 2:1, as specified by the manufacturer, to ultimately create a highly cross-linked polymer. Spherical, pure titanium powder (>99.9% purity, 0-45 μm, manufactured by Raymor, Canada), shown in the scanning electron microscopy (SEM) image in Figure 1(a), was used

as the base powder. Spherical powder was used in preference to irregularly shaped powders due to its superior flowability. The titanium powder was mixed with the epoxy binder in an 8:1 weight ratio to create a paste. Samples with height of 12 mm and diameter of 6 mm were directly extruded for both materials characterization and compression tests. Sintering was carried out in a high vacuum tube furnace (Carbolite-Gero, STF 15) at 1250 °C for 2 hrs with a vacuum pressure of 10^{-5} Torr. All samples were placed on an alumina ceramic substrate during sintering. The furnace was heated, then isothermally held at 350 °C for 1 hour before heating at 4 °C/min to the sintering temperature of 1250 °C. The polymer is removed by burnt out during heating. Samples were furnace-cooled to room temperature at a rate of 4 °C/min.

2.2 Density and porosity measurement

The density and open porosity of the sintered samples was determined by the Archimedes method with oil impregnation. H-Galden ZT-180 was used as the immersion fluid in preference to water to give more accurate results. The density of the sintered sample, ρ, and porosity P_{Open} , were calculated using:

$$\rho = \frac{\rho_{HG} \times W_{Air}}{W_{Oil} - W_{HG}}$$

(1)

$$P_{Open} = \frac{\rho_{HG}(W_{Oil} - W_{Air})}{\rho_{Oil}(W_{Oil} - W_{HG})} \times 100$$

(2)

where ρ_{HG} is the density of the H-Galden (1.69 g/mL at 21°C), ρ_{Oil} is the density of the oil (KS7470, density 0.885 g/mL), W_{Air} is the dry weight of the compact, W_{Oil} is the weight of the compact after oil infiltration, and W_{HG} is the weight of the oil infiltrated compact

measured while immersed in H-Galden. The pore interconnectivity was assessed from the ratio of the open to total porosity (general porosity) [25].

2.3 Microstructural and mechanical characterization

The mechanical properties of the porous titanium scaffolds were measured by compression tests following the ASTM E9 standard. The tests were carried out in triplicate using an Instron 5584 test machine, with cylindrically shaped samples 12 mm in height and 6 mm in diameter. Samples were prepared using precision CNC machining for geometrical accuracy. Tests were conducted with a cross-head speed of 0.001 mm/s at room temperature. Each test sample was loaded until fracture. The elastic modulus, ultimate compressive strength, yield strength and strain at fracture were measured. The 0.2%-offset proof strength was taken to approximate yield strength.

Specimens for microstructural investigation were cross-sectioned and mounted in epoxy resin. Mounted specimens were ground on progressively finer SiC paper to 1200 grit and polished with a mixture of colloidal silica and H_2O_2 with a 9:1 volume ratio. SEM analysis was performed using a Hitachi Tabletop Scanning Electron Microscope (SEM, TM3030) with a 5kV accelerating voltage using secondary electron imaging mode.

2.4 Assessment of the *in-vitro* bioactivity

2.4.1 Sample preparation

Titanium disks (10 mm diameter; 1 mm thick) were sliced from sintered samples using a Struers Accutom Cut-off saw with a diamond cutting disk (0.8mm thick). A cutting speed of 2000 rpm and a cutting rate of 0.025 mm/s was chosen to generate fine sectioned surfaces with intact open pore structures without the requirement for further polishing. The disks were

then cleaned in an ultrasonic cleaner, immersed in acetone, for 20 mins. The disks were subsequently rinsed with deionized water and dried under vacuum. The disks were individually wrapped in gauze to prevent damage and sterilized by autoclaving (121°C for 20 mins, and dried at 65°C).

2.4.2 Mesenchymal stem cell culture

Human bone-marrow-derived Mesenchymal Stem Cells (hMSCs, RoosterBio) were cultured in DMEM low glucose media supplemented with 100 U/mL penicillin, 100 µg/mL streptomycin and 10% fetal bovine serum (FBS) at 37 °C with 5% CO_2. Upon reaching 80% confluence, the cells were passaged and replated on the scaffolds at a density of 10,000 cells/cm^2. Cells at passage 4-6 were used in this study.

2.4.3 Cell proliferation

Cell viability was assessed by 3-(4,5-dimethylthiazol-2yl)-2,5-diphenyltetrazolium bromide (MTT) assay using the protocols described in [26] by Han *et al*. hMSC viability was measured after culturing for 1 and 7 days, using triplicates for each condition. To quantify cell viability, 0.5 mg/mL of MTT solution (sourced from Sigma-Aldrich) was added to each well of the tissue culture plate and incubated at 37 °C for 4 hours to form formazan crystals. The formazan was solubilized with dimethyl sulfoxide and the absorbance assessed at 495 nm in a 96-well plate reader.

2.4.4 hMSC attachment and focal adhesion analysis

Prior to seeding, the scaffolds were sterilised by means of autoclave at 121°C for 21 mins, and dried at 65°C in an oven. hMSCs were detached with TrypLE Select (Invitrogen), resuspended in DMEM/10%FBS/1%PS by volume and seeded onto the scaffolds at a density of 10,000 cells/cm^2. After 4 and 24 hours of culturing the samples were rinsed gently with PBS and fixed in 4 vol % paraformaldehyde for 10 minutes at room temperature (RT). After

fixation, the samples were rinsed with PBS for 5 minutes at RT. After blocking with 1 vol % goat serum in PBS for 1 hr, the primary antibody of mouse-anti-human vinculin was incubated at RT for 1 hour, followed by incubation with a goat-anti-mouse 568 secondary antibody for 1 hour containing Alexa Fluor 488 Phalloidin and Hoechst 33342. After rinsing with 0.1 vol % Tween/PBS, the cells were imaged using a Zeiss 710 confocal microscope.

2.4.5 Statistical analysis

All cellular experiments were performed in triplicates. Data is presented as the mean value standard error of the mean analysed with a student t-test. Statistical significance was considered at $p < 0.05$.

3. Results and Discussion

3.1 Structure observation

The thermoset polymer ink allows the scaffold to hold its shape during sintering and leaves a porous structure after its removal during sintering. Figure 1(A) shows the morphology of the spherical pure titanium powder with size range of 0-45 µm used in this study. Figure 1(B) shows an SEM image of a polished cross-section of the scaffolds revealing pore size, morphology and distribution. As shown in Figure 1(C), pores are around 200-500 µm in size and within the preferred size range to promote cell osseointegration [14]. The pores are generally elongated in shape and evenly distributed across the scaffold cross section. The pore walls have smooth curvatures and interconnectivity can be observed between the pores. The degree of interconnectivity will be assessed through the porosity measurements.
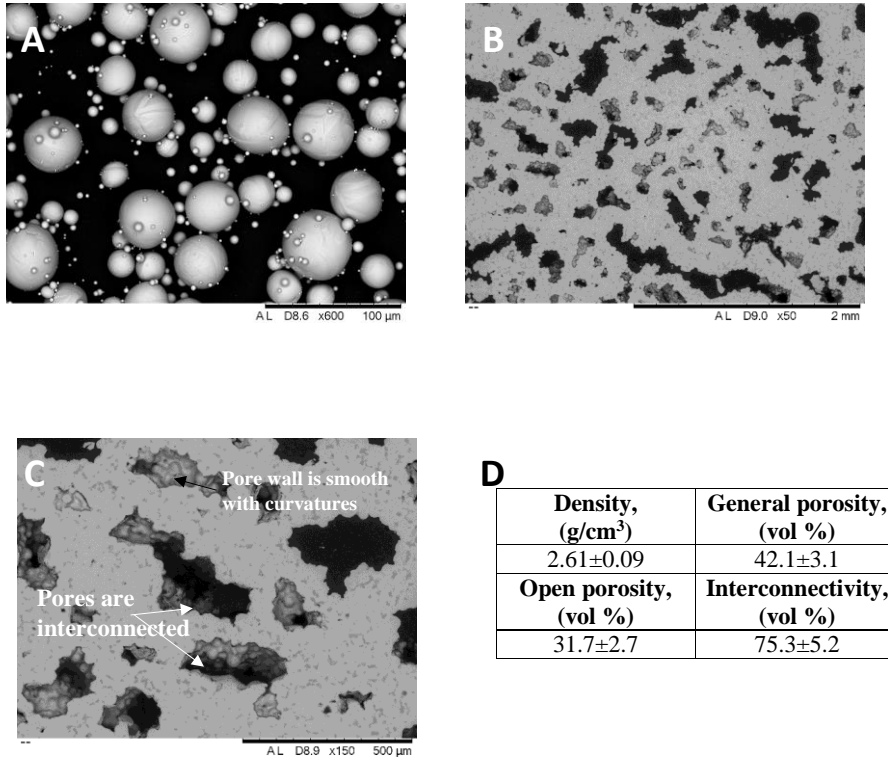
Density, (g/cm^3)	General porosity, (vol %)
2.61±0.09	42.1±3.1
Open porosity, (vol %)	**Interconnectivity, (vol %)**
31.7±2.7	75.3±5.2

Figure 1. SEM images (A, B, C) showing (A) The morphology of the spherical pure titanium powder used in this study, (B) Pore sizes and distribution on a cross-section of the sintered sample, (C) Higher magnification of the pore morphologies, and (D) the measured density, porosities and interconnectivity.

Figure 1(D) shows the measured density and corresponding porosities of the sintered material. The density is 2.61 g/cm^3, which is almost half that of pure titanium (4.506 g/cm^3). Density can be controlled by changing the polymer-metal powder ratio and the porosity can be further modified through designed porous structures. Healthy human bone mineral density (BMD) on average is around 3.88 g/cm^3 in males and 2.90 g/cm^3 in females. Density, consistent with the

BMD range, can improve patient comfort and reduce rates of implant failure [27]. It should be noted that the porosity of 42.1 vol % is ideally suited to biomaterial applications as the optimal range for implant materials is considered 30–90 vol % [28]. The pore interconnectivity was assessed from the ratio of open to total porosity (general porosity) [25], which demonstrates that the pores are highly interconnected (above 70%).

3.2 Mechanical properties

A
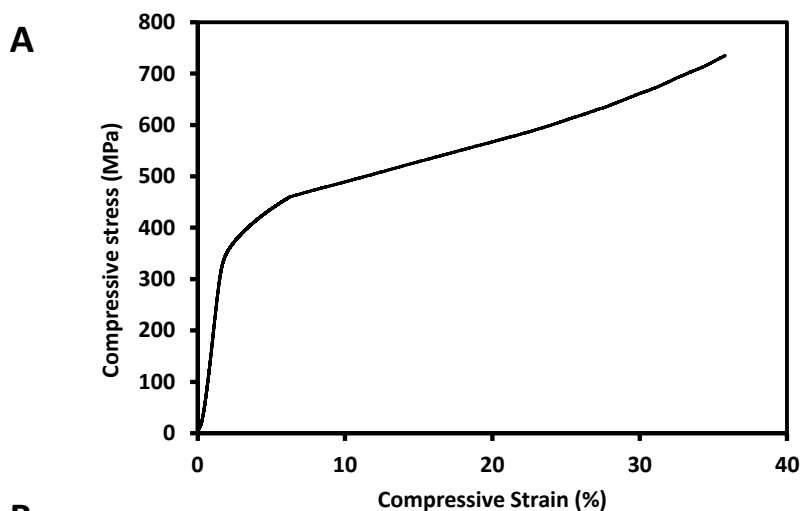
	$\sigma_{0.2}$ (MPa)	σ_{30} (MPa)	Young's Modulus (GPa)
DIW porous Ti	340 ± 15	660 ± 23	20.2 ± 2
PM 40% porous Ti [14]	221.7 ± 17.5	301.7 ± 10	24.7 ± 2.5
Human Cortical Bone [29]	104-121	-	4-30
Selective Laser Melting Ti Scaffold [30]	-	-	77 ± 3.5
Eletron Beam Melting Ti-6Al-4V scaffolds [19]	24.3 ± 0.4	-	842 ± 11 (MPa)
DIW Hardystonite Scaffolds [31]	2.5 ± 0.6	-	-
DIW Bioactive Glass Scaffolds [32]	136 ± 22	-	2
DIW Scaffolds with	11 ± 5.4 (β-TCP)	26 (β-TCP)	-

B

colloidal calcium phosphates inks [33]	15 ± 6.9 (BCP)	36 (BCP)	

Figure 2: (A) Representative compressive stress-strain curve for the porous Ti and (B) corresponding mechanical properties and several different materials from references with mean ± standard deviation for comparison.

Mechanical properties of the DIW porous titanium samples are presented in Figure 2 with (A) showing a representative stress-strain curve under compression loading and (B) showing the average mechanical properties including the 0.2% yield strength ($\sigma_{0.2}$), compressive strength at 30% compression (σ_{30}) and the Young's modulus. For comparison, the properties of human cortical bone, porous titanium scaffold produced through powder metallurgy with a similar porosity level (40%), scaffolds produced by Direct Ink Writing and metallic 3D printing are also shown in Figure 2(B). Compared to porous scaffold manufactured by metallic 3d printing such as Selective Laser Melting [30] and Electron Beam Melting [19], the effective Young's modulus of the porous DIW processed titanium samples is relatively low and within the range of that of human cortical bone, curtailing any potential "stress shielding" effects [14]. Meanwhile, the strength of the samples is significantly greater than that of human cortical bone [14]. Both the 0.2% yield strength ($\sigma_{0.2}$) and compressive strength at 30% compression (σ_{30}) are superior to those of porous titanium scaffolds manufactured through standard powder metallurgy techniques employing a space holder approach [13,34] and ceramic scaffolds produced using DIW techniques [31–33]. These promising results show the suitability of the porous titanium samples manufactured by the DIW for implant applications. The implants effectively mimic the elastic modulus of human bone whilst possessing a high yield strength to resist permanent deformation under loading [34].

3.3 hMSCs proliferation, morphology and adhesion

To gauge biocompatibility of the titanium scaffolds, an MTT assay was conducted to assess the viability and proliferation of hMSCs against tissue culture plate (TCP) controls after 1 and 7 days of culture. The MTT assay results, as shown in Figure 3, showed that the viability of the cells on all scaffolds was significantly higher than TCP. The titanium scaffolds out-performed those produced with similar porosity (40%) by powder metallurgy [14] which show a significantly lower cell viability (lower than TCP) after 1 day of culture. This is believed to be due to the particular characteristics of the porous structures in the respective scaffolds, in particular the pore shape, pore interconnectivity and surface roughness, and is the subject of further more detailed investigations. The current results demonstrate that the DIW scaffolds actively promote cell proliferation.
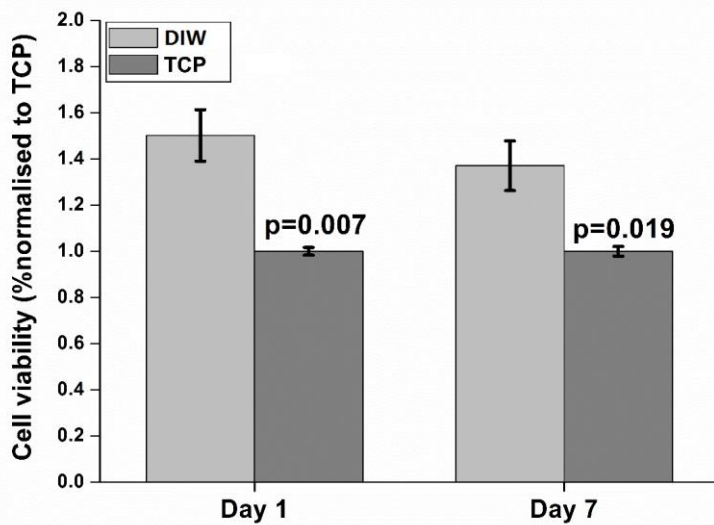
Figure 3. hMSC viability on DIW porous Ti and TCP from MTT assay of after 1 and 7 days culture. Data is presented as absorbance normalised to TCP controls with mean± s.e.m. for n=3.

To evaluate cell compatibility and responses on the DIW processed scaffolds, scaffold samples were seeded with hMSCs for 4 and 24 hrs. Cell morphology analysis was used to assess the attachment of the seeded cells and actin microfilaments are the major structural element for evaluation. Fluorescent imaging (Figure 4a) shows the morphology of hMSCs on the DIW scaffold at both 4 and 24 hrs. The images show that the cells initiate interaction with the underlying substrate with well-spread morphologies at both time points. The cells proliferate in number and actin microfilament networks were well-developed overtime. Large, well-defined stress fibres can be observed at both time points. Actin cytoskeleton are also well-organized. There are no discernible differences between TCP and the scaffold surfaces, which indicates the high biocompatibility of the scaffolds.
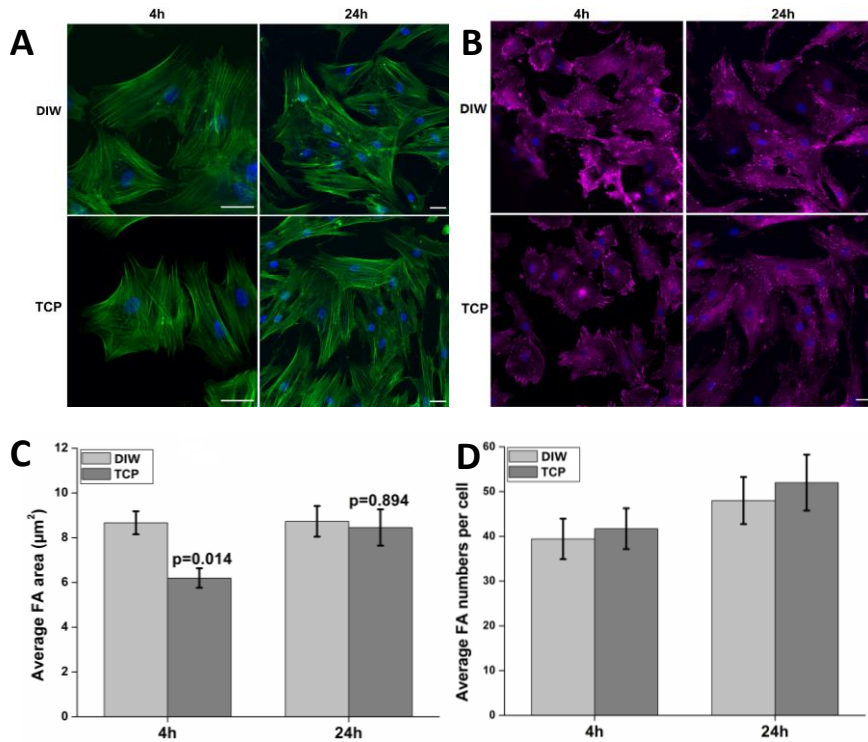
Figure 4. Evaluation of cell attachment and morphology on DIW porous Ti scaffolds and comparisons to TCP. (A) Cell attachment and morphology using F-actin (green) and nucleus (blue). Scale bar = 50um. (B) Vinculin expression on hMSCs after 4 hr and 24 hr of culture. Pink (vinculin) and nucleus (blue). Scale bar = 50um. (C) Quantification of average FA area and (D) numbers per cell (n=30).

The influence of the DIW porous scaffolds on adhesion and spreading of hMSCs was also investigated. Changes to the cytoskeletal architecture, in particular to Focal adhesion (FA) formation were examined. FA are complex protein arrays that produce, transmit and sense mechanical tension [35] and play an important role in cell migration. FAs were used as an indication of cell adhesion and spreading. Vinculin is a membrane-cytoskeletal protein in FAs that is involved in linkage of integrin adhesion molecules to the actin cytoskeleton.

Vinculin fluorescent immunohistological staining was utilised to detect matrix adhesion to discrete vinculin-positive complexes after 4 and 24 hours culture. At both 4 and 24 hr, hMSCs had large, discrete vinculin-positive complexes, localized to the ends of the actin filaments on the scaffolds samples (Figure 4B), with equivalent FA numbers to that of the TCP (Figure 4D). Measurements of the vinculin areas determined that hMSCs on DIW porous scaffolds had a significantly larger FA area compared to the TCP control, indicative of fully mature FAs after 4 hrs culture (Figure 4 C&D). There were no statistically significant differences with FA numbers between any of the samples at both time points. These results demonstrate that the DIW porous Ti scaffolds support viability and attachment of hMSCs.

4. Conclusion

Direct Ink Writing (DIW) of titanium scaffolds is a promising and innovative solution to waste free 3D printing of net shape complex parts. In our study, we have demonstrated a novel biocompatible DIW ready binder and investigated its feasibility for manufacturing porous titanium scaffolds for orthopaedic applications. A thermosetting polymer was mixed with spherical titanium powder to generate green parts. The polymer was subsequently burnt out during sintering to form scaffolds containing elongated pores with a high degree of interconnectivity (>70%). The elastic moduli of the scaffolds was ~20.2 GPa for a porosity of ~42%, which is within the typical range of human cortical bone (4-30 GPa), whilst the yield strength ($\sigma_{0.2} = 340$ MPa) far exceeded that of human bone (130-180 MPa). Evaluation using in-vitro human bone-marrow-derived MSC (hMSCs) cell line showed that the cells exhibited a well-spread morphology and excellent adhesion to the sample surfaces, while the MTT assay cell viability results have established that all samples were highly biocompatible and superior to that of tissue culture controls. This research demonstrates the excellent potential for the use of a thermosetting polymer binder for titanium DIW, and in particular, the

applicability of this technique to the manufacture of porous scaffolds for hard tissue engineering.

Acknowledgment

Reference

[1]   F.J. O'Brien, Biomaterials & scaffolds for tissue engineering, Mater. Today. 14 (2011) 88–95. doi:10.1016/S1369-7021(11)70058-X.

[2]   A.T. Jensen, S.S. Jensen, N. Worsaae, Complications related to bone augmentation procedures of localized defects in the alveolar ridge. A retrospective clinical study, Oral Maxillofac. Surg. 20 (2016) 115–122. doi:10.1007/s10006-016-0551-8.

[3]   E. Nkenke, F.W. Neukam, Autogenous bone harvesting and grafting in advanced jaw resorption: morbidity, resorption and implant survival., Eur. J. Oral Implantol. 7 Suppl 2 (2014) S203-17. http://www.ncbi.nlm.nih.gov/pubmed/24977256 (accessed October 27, 2017).

[4]   M. Geetha, A.K. Singh, R. Asokamani, A.K. Gogia, Ti based biomaterials, the ultimate choice for orthopaedic implants - A review, Prog. Mater. Sci. 54 (2009) 397–425. doi:10.1016/j.pmatsci.2008.06.004.

[5]   D. Kent, G. Wang, Z. Yu, X. Ma, M. Dargusch, Strength enhancement of a biomedical titanium alloy through a modified accumulative roll bonding technique, J. Mech. Behav. Biomed. Mater. 4 (2011) 405–416. doi:10.1016/j.jmbbm.2010.11.013.

[6]   Y. Zhang, D. Kent, G. Wang, D. St John, M. Dargusch, Evolution of the microstructure and mechanical properties during fabrication of mini-tubes from a biomedical β-titanium alloy, J. Mech. Behav. Biomed. Mater. 42 (2015) 207–218. doi:10.1016/j.jmbbm.2014.11.013.

[7]   A. Nouri, P.D. Hodgson, C. Wen, Biomimetic Porous Titanium Scaffolds for, in: 2010: pp. 415–450.

[8]   J.P. Li, J.R. De Wijn, C.A. Van Blitterswijk, K. De Groot, Porous Ti6Al4V scaffold directly fabricating by rapid prototyping: Preparation and in vitro experiment, Biomaterials. 27 (2006) 1223–1235. doi:10.1016/j.biomaterials.2005.08.033.

[9]   S. Maleksaeedi, J.K. Wang, A. El-Hajje, L. Harb, V. Guneta, Z. He, F.E. Wiria, C. Choong, A.J. Ruys, Toward 3D printed bioactive titanium scaffolds with bimodal pore size distribution for bone ingrowth, Procedia CIRP. 5 (2013) 158–163. doi:10.1016/j.procir.2013.01.032.

[10]   B. Wysocki, J. Idaszek, K. Szlązak, K. Strzelczyk, T. Brynk, K. Kurzydłowski, W. Święszkowski, Post Processing and Biological Evaluation of the Titanium Scaffolds

for Bone Tissue Engineering, Materials (Basel). 9 (2016) 197. doi:10.3390/ma9030197.

[11] N.G. Davis, J. Teisen, C. Schuh, D.C. Dunand, Solid-state foaming of titanium by superplastic expansion of argon-filled pores, J. Mater. Res. 16 (2001) 1508–1519. doi:10.1557/JMR.2001.0210.

[12] L.D. Zardiackas, D.E. Parsell, L.D. Dillon, D.W. Mitchell, L.A. Nunnery, R. Poggie, Structure, metallurgy, and mechanical properties of a porous tantalum foam., J. Biomed. Mater. Res. 58 (2001) 180–7. http://www.ncbi.nlm.nih.gov/pubmed/11241337 (accessed July 21, 2017).

[13] Y. Chen, D. Kent, M. Bermingham, A. Dehghan-Manshadi, M. Dargusch, Manufacturing of biocompatible porous titanium scaffolds using a novel spherical sugar pellet space holder, Mater. Lett. 195 (2017) 92–95. doi:10.1016/j.matlet.2017.02.092.

[14] Y. Chen, J.E. Frith, A. Dehghan-Manshadi, H. Attar, D. Kent, N.D.M. Soro, M.J. Bermingham, M.S. Dargusch, Mechanical properties and biocompatibility of porous titanium scaffolds for bone tissue engineering, J. Mech. Behav. Biomed. Mater. 75 (2017) 169–174. doi:10.1016/j.jmbbm.2017.07.015.

[15] Y. Wang, Y. Shen, Z. Wang, J. Yang, N. Liu, W. Huang, Development of highly porous titanium scaffolds by selective laser melting, Mater. Lett. 64 (2010) 674–676. doi:10.1016/j.matlet.2009.12.035.

[16] L. Hirt, A. Reiser, R. Spolenak, T. Zambelli, Additive Manufacturing of Metal Structures at the Micrometer Scale, Adv. Mater. 29 (2017) 1604211. doi:10.1002/adma.201604211.

[17] L.-C. Zhang, H. Attar, Selective Laser Melting of Titanium Alloys and Titanium Matrix Composites for Biomedical Applications: A Review , Adv. Eng. Mater. 18 (2016) 463–475. doi:10.1002/adem.201500419.

[18] D. Zhang, C.S. Wong, C. Wen, Y. Li, Cellular responses of osteoblast-like cells to 17 elemental metals, J. Biomed. Mater. Res. - Part A. 105 (2017) 148–158. doi:10.1002/jbm.a.35895.

[19] A. Ataee, Y. Li, D. Fraser, G. Song, C. Wen, Anisotropic Ti-6Al-4V gyroid scaffolds manufactured by electron beam melting (EBM) for bone implant applications, Mater. Des. 137 (2018) 345–354. doi:10.1016/J.MATDES.2017.10.040.

[20] J.A. Slotwinski, E.J. Garboczi, P.E. Stutzman, C.F. Ferraris, S.S. Watson, M.A. Peltz, Characterization of Metal Powders Used for Additive Manufacturing, J. Res. Natl. Inst. Stand. Technol. 119 (2014) 460. doi:10.6028/jres.119.018.

[21] J.A. Lewis, Direct Ink Writing of 3D Functional Materials, Adv. Funct. Mater. 16 (2006) 2193–2204. doi:10.1002/adfm.200600434.

[22] L. Fiocco, H. Elsayed, D. Badocco, P. Pastore, D. Bellucci, V. Cannillo, R. Detsch, A.R. Boccaccini, E. Bernardo, Direct ink writing of silica-bonded calcite scaffolds from preceramic polymers and fillers, Biofabrication. 9 (2017) 025012. doi:10.1088/1758-5090/aa6c37.

[23] Lewis, Novel Inks for Direct-Write Assembly of 3-D Periodic Structures, Mater. Matters. 3 (2008). https://lewisgroup.seas.harvard.edu/publications/novel-inks-direct-write-assembly-3-d-periodic-structures (accessed July 21, 2017).

[24] A.E. Jakus, E.B. Secor, A.L. Rutz, S.W. Jordan, M.C. Hersam, R.N. Shah, Three-Dimensional Printing of High-Content Graphene Scaffolds for Electronic and Biomedical Applications, ACS Nano. 9 (2015) 4636–4648. doi:10.1021/acsnano.5b01179.

[25] M.P. Albano, L.B. Garrido, K. Plucknett, L.A. Genova, Processing of porous yttria-stabilized zirconia tapes: Influence of starch content and sintering temperature, Ceram. Int. 35 (2009) 1783–1791. doi:10.1016/J.CERAMINT.2008.10.003.

[26] P. Han, S. Ivanovski, R. Crawford, Y. Xiao, Activation of the Canonical Wnt Signaling Pathway Induces Cementum Regeneration, J. Bone Miner. Res. 30 (2015) 1160–1174. doi:10.1002/jbmr.2445.

[27] L. Molly, Bone density and primary stability in implant therapy., Clin. Oral Imp. Res. 12 (2006) 124–13.

[28] S. Sobieszczyk, Optimal Features of Porosity of Ti Alloys Considering their Bioactivity and Mechanical Properties, Adv. Mater. Sci. 10 (2010) 20–30. doi:10.2478/v10077-010-0007-z.

[29] P. Lichte, H.C. Pape, T. Pufe, P. Kobbe, H. Fischer, Scaffolds for bone healing: Concepts, materials and evidence, Injury. 42 (2011) 569–573. doi:10.1016/j.injury.2011.03.033.

[30] T. Traini, C. Mangano, R.L. Sammons, F. Mangano, A. Macchi, A. Piattelli, Direct laser metal sintering as a new approach to fabrication of an isoelastic functionally graded material for manufacture of porous titanium dental implants, Dent. Mater. 24 (2008) 1525–1533. doi:10.1016/J.DENTAL.2008.03.029.

[31] A. Zocca, G. Franchin, H. Elsayed, E. Gioffredi, E. Bernardo, P. Colombo, A. Bandyopadhyay, Direct Ink Writing of a Preceramic Polymer and Fillers to Produce Hardystonite (Ca2ZnSi2O7) Bioceramic Scaffolds, J. Am. Ceram. Soc. 99 (2016) 1960–1967. doi:10.1111/jace.14213.

[32] Q. Fu, E. Saiz, A.P. Tomsia, Direct ink writing of highly porous and strong glass scaffolds for load-bearing bone defects repair and regeneration, Acta Biomater. 7 (2011) 3547–3554. doi:10.1016/j.actbio.2011.06.030.

[33] R.C. Richard, R.N. Oliveira, G.D.A. Soares, R.M.S.M. Thiré, Direct-write assembly of 3D scaffolds using colloidal calcium phosphates inks, in: Rev. Mater., 2014: pp. 61–67. doi:10.1590/S1517-70762014000100009.

[34] M. Niinomi, Recent research and development in titanium alloys for biomedical applications and healthcare goods, Sci. Technol. Adv. Mater. 4 (2003) 445–454. doi:10.1016/j.stam.2003.09.002.

[35] K. Burridge, C. Guilluy, Focal adhesions, stress fibers and mechanical tension, Exp. Cell Res. 343 (2016) 14–20. doi:10.1016/j.yexcr.2015.10.029.